



CHORUS

This is the accepted manuscript made available via CHORUS. The article has been published as:

## High-harmonic spectroscopy of laser-driven nonadiabatic electron dynamics in the hydrogen molecular ion

M. R. Miller, A. Jaroń-Becker, and A. Becker

Phys. Rev. A **93**, 013406 — Published 11 January 2016

DOI: [10.1103/PhysRevA.93.013406](https://doi.org/10.1103/PhysRevA.93.013406)

# High harmonic spectroscopy of laser driven nonadiabatic electron dynamics in the hydrogen molecular ion

M. R. Miller,<sup>1</sup> A. Jaroń-Becker,<sup>1</sup> and A. Becker<sup>1</sup>

<sup>1</sup>*JILA and Department of Physics, University of Colorado, Boulder, CO 80309-0440, USA*

We theoretically explore a new mechanism resulting in a minimum in the high harmonic spectrum of a hydrogen molecular ion driven at extended internuclear distances by a mid-infrared laser source. Our analysis identifies this minimum to be a signature of the transient localization of the electron upon alternating nuclear centers and is representative of dynamics occurring exclusively at the time of ionization. We further demonstrate the sensitivity of this spectroscopic feature to driving field parameters as well as its robustness to distributions of laser field intensities and internuclear distances. Finally, we show how variations in the nonadiabatic dynamics induced by the ramping driving field can be imaged through changes in the number and locations of minima in the spectra.

## I. INTRODUCTION

Observing the time-resolved behavior of electrons is among the primary challenges at the frontier of attosecond science (1 as =  $10^{-18}$  s) [1]. Attosecond temporal resolution of electron dynamics can be achieved via high harmonic generation (HHG) through the interaction of atoms and molecules with intense femtosecond lasers [2]. It involves the release of an electron wavepacket into the continuum through tunneling, followed by its laser-driven propagation away from and then back towards the parent ion [3–5]; upon recombination, HHG with photon energies extending to the soft-X-ray region [6] is generated. Each of the three steps (emission, propagation and recombination) occurs on a femto- or sub-femtosecond time span. HHG is therefore a natural spectroscopic tool [7] and has been used to time resolve vibrational wave packet dynamics [8–11], adiabatic electron wave packet motion in bound states of a molecule [12–14], and the dynamics in excited electronic states during photodissociation [15–17].

Molecules serve as a fascinating source for HHG, as dynamical or structural effects during any step of HHG may significantly influence the resultant spectrum, in particular by imprinting minima at specific harmonic orders. Structural interference minima have been theoretically [18–20] and experimentally [8–11, 21–26] studied as a means of probing molecular structures and nuclear dynamics by defining a criterion analogous to two-center interference. In contrast, dynamical minima occur when the temporal evolution of the system results in a phase difference between propagating and residual electron wavepackets. This is, for example, the case when multiple molecular orbitals are energetically close to the continuum and are thus allowed to tunnel through the potential barrier in the first step of HHG. The residual molecular ion remains in a coherent superposition of the ground and excited states which accumulate a destructive phase difference with the returning wavepacket for suitable excursion times [13–17].

Common between these mechanisms is the importance of the wavepacket recombination to the exhibition of spectral minima. In fact, past investigations of the role

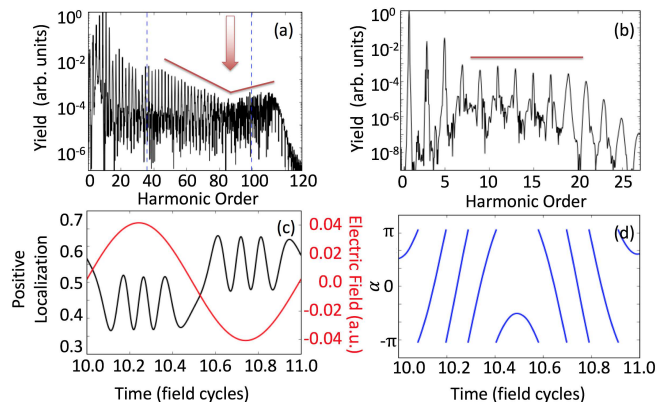


FIG. 1. (Color online) (a) Driving extended ( $R_0 = 7$ )  $H_2^+$  with 1.8  $\mu\text{m}$  midinfrared light results in a minimum in the HHG spectrum (indicated by the superimposed red lines for the overall structure and the red arrow for the spectral location of the minimum). This minimum is notable in comparison with (the expected) consistent yield throughout the plateau generated with a 0.8  $\mu\text{m}$  light source in (b). The manifestation of the minimum (a) coincides with sub-cycle transient localization of the electron upon alternating nuclear centers, demonstrated (c) throughout one laser cycle (red line) by the integrated electron density occupying  $z > 0$  (black line), and resulting from (d) the evolving relative phase difference between the wavefunction centered on each nucleus.

played by ionization and recombination matrix elements in the formation of structurally indicative HHG minima have shown that ionization plays a negligible role in the creation of these minima. Surprisingly, in the following we identify a minimum in theoretical predictions for the HHG of  $H_2^+$  which is distinct from previously explored mechanisms in that its spectral location is predicated entirely upon electron dynamics at the time of ionization.

## II. HIGH-ORDER HARMONIC GENERATION OF EXTENDED $H_2^+$

An example is shown in Fig. 1 (a) for  $H_2^+$  prepared in its ground state with internuclear distance  $R_0 = 7$  a.u.,

driven by a 20 cycle full-width mid-infrared (IR) laser pulse with wavelength  $\lambda = 1.8 \mu\text{m}$  and peak intensity  $6 \times 10^{13} \text{ Wcm}^{-2}$ . In contrast to the flat plateau structure observed when driving with a shorter wavelength (Fig. 1 (b)), for the midinfrared driver the HHG plateau is modulated, accompanied by peak suppression at the 87th harmonic order. The location of the minimum in the spectrum cannot be explained as a structural two-center interference minimum, which would cause suppression at energies indicated by the dashed lines in Fig. 1(a) [18, 19]. This finding is in agreement with the predicted absence of structural minima for systems at extended internuclear distances [29]. Since  $\text{H}_2^+$  is a single-electron system, this minimum must also be distinct from dynamical minima arising from other (e.g. multi-electron effects) effects. [13]. As we discuss below, its presence is instead solely predicated on the laser-driven nonadiabatic electron dynamics at the time of ionization [28, 30–32]. In  $\text{H}_2^+$ , nonadiabatic dynamics occurs due to the near degeneracy of the  $|g\rangle$  and  $|u\rangle$  states at extended internuclear distances. Nonadiabatic dynamics also plays an important role in polyatomic molecules interacting with intense laser fields [27, 33–35]. Studying the simplest molecule  $\text{H}_2^+$  offers the opportunity to focus upon the spectroscopic signatures of nonadiabatic dynamics, disentangled from multi-electron effects.

### A. Computational methods

Calculations were performed for a fixed-nuclei model of  $\text{H}_2^+$  exposed to a linearly polarized laser field by solving the time-dependent Schrödinger equation (TDSE) for electron motion in three dimensions using a standard Crank-Nicholson method. Alignment of the internuclear axis with the laser polarization direction was assumed, and the time-dependent wavefunction was obtained to compute HHG spectra as the Fourier transform of the dipole acceleration. The Hamiltonian for this system ( $e = \hbar = m = 1$ ) is given by

$$H(t) = -\frac{1}{2}\left(\frac{1}{\rho}\frac{\partial}{\partial\rho}\rho\frac{\partial}{\partial\rho} + \frac{\partial^2}{\partial z^2}\right) - \frac{1}{\sqrt{\rho^2 + (z + \frac{R_0}{2})^2}} - \frac{1}{\sqrt{\rho^2 + (z - \frac{R_0}{2})^2}} + zE(t), \quad (1)$$

where  $R_0$  is the internuclear distance of the molecular ion, and  $E(t) = E_0 \cos(\omega t) \sin^2(\pi t/N\tau)$  is the electric field. Grid spacings of  $\Delta z = 0.1$  a.u. and  $\Delta\rho = 0.0375$  a.u. were used, along with a time step  $\Delta t = 0.01$  a.u.; the total numerical grid occupied 400 points (15 a.u.) in the  $\rho$  direction and was adjusted in the  $z$  direction to exceed four times the electron quiver radius in each calculation.

### B. Transient electron localization

Nonadiabatic electron dynamics manifests itself via more than one localization on each nuclei per half laser field cycle. The transfer of electron population between nuclear centers is mediated by the intrinsic two-center interference in  $\text{H}_2^+$ , gating the momentum of the electron as it travels across the molecule [31]. The position of this momentum gate depends on the strength of the electric field, which can lead to electron motion against the driving field gradient, hence a nonadiabatic electron dynamics, and consequently a population of the counter-intuitive side of the molecule.

Numerically, this behavior can be captured by recording asymmetries in the electron distribution along the internuclear spatial dimension and is shown in Fig. 1(c), in which the radially-integrated relative population of the  $z > 0$  section of the spatial grid is displayed. Throughout one middle cycle of the driving laser field, it can be seen that the electron transiently localizes upon alternating nuclei several times per half cycle, in contrast to the intuitive single instance per half cycle expected of an adiabatically laser driven system. The nonadiabatic dynamics is closely related to the time-dependent difference in the phase of the electron wavefunction  $\Psi(\rho, z; t)$  near each of the protons [36]

$$\alpha(t) = \arg\left[\Psi\left(\frac{\Delta\rho}{2}, \frac{R_0}{2}; t\right)\right] - \arg\left[\Psi\left(\frac{\Delta\rho}{2}, -\frac{R_0}{2}; t\right)\right], \quad (2)$$

Comparing results in Fig. 1(c) and (d), we see that at instants when  $\alpha = 0$ , the electron is localized upon the upper potential well within the molecule related to a suppression in electron emission. Instants of maximal spatial localization are predicted to satisfy [31]

$$A(t_{loc}) = \frac{m\pi + \chi}{2|g|z|u|}, \quad (3)$$

where  $\chi$  is a mixing angle between Floquet states reducing to  $|g\rangle$  and  $|u\rangle$  at zero field intensity (for a system prepared initially in its ground state,  $\chi = 0$ ),  $m$  is an integer satisfying  $m \in \mathbb{Z}$ , and assuming a driving electric field  $E(t) = -E_0 \cos(\omega t + \phi)$  with  $A(t) = -\int E(t)dt$ , approximating conditions at the peak of the driving field. Eq. (3) shows that the number of incidences of localization per laser cycle can be increased by using a laser source with higher intensity or longer wavelength.

### III. THE ROLE OF TRANSIENT LOCALIZATION IN HHG

To proceed, we seek to connect the nonadiabatic dynamics and sub-cycle transient localization of the electron with the emission of radiation from the system. It is known that the nonadiabatic transient localization results in several distinct bursts of ionization throughout

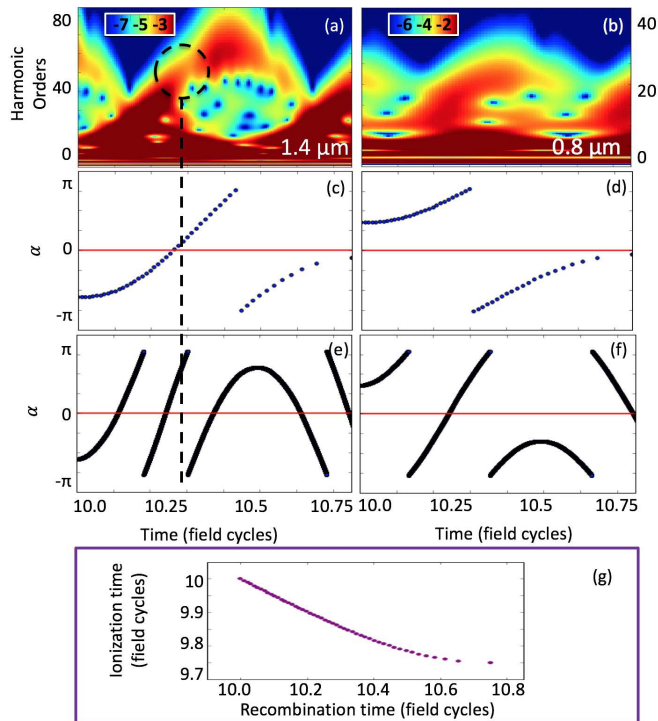


FIG. 2. (Color online) Wavelet analyses of the electron dipole acceleration throughout recombination spanning 10.0 – 10.75 field cycles driven by a 1.4  $\mu\text{m}$  (a) reveals intervals of reduced harmonic emission (black dashed circle), in contrast to the constant efficiency of emission between 10 – 10.5 field cycles found when driving using a 0.8  $\mu\text{m}$  (b) laser source. Electron behavior is represented using  $\alpha$  during the classically reconstructed time of ionization (c,d) and during recombination (e,f). (g) Relation via a classical model [3] between ionization and recombination times.

each half-cycle of the driving field, predicted theoretically [31] and corroborated by indirect measurement of the ionization time delay probed by circularly polarized light [32]. These bursts of ionization are notably separated by instants of suppressed wavepacket emission, corresponding to solutions of Eq. (3) for even  $m$ . This potentially provides a cause for the observed harmonic minimum, since the first step of harmonic generation relates to the emission of the wavepacket.

### A. Time-frequency analysis

As the full HHG spectrum provides no temporal resolution, we employ the continuous wavelet analysis

$$C(t_0, \omega) = \frac{1}{\sqrt{2\pi}} \int_0^T d a_z(t) W\left(\frac{\omega(t-t_0)}{2\pi}\right) dt, \quad (4)$$

where  $W(x) = \frac{1}{\sqrt{\pi}} \exp(2\pi i x) \exp(-x^2)$  is the complex Morlet wavelet. In Fig. 2 we demonstrate the use of the wavelet transform to resolve harmonic emission throughout a single rescattering event near the peak of the driv-

ing field using wavelengths of 1.4  $\mu\text{m}$  (a) and 0.8  $\mu\text{m}$  (b). In each case, the wavelet picture provides HHG emission throughout 10.0 – 10.75 field cycles, corresponding to ionization events between 9.75 – 10.0 field cycles. For the 1.4  $\mu\text{m}$  case, we note with a dashed circle an interval of suppressed harmonic emission, matching the spectral position of the minimum in the full HHG spectrum. To understand the source of the minimum, we examine the evolution of the wavepacket during ionization and recombination time intervals contributing to the HHG.

Harmonic emission occurs at the time of electron recombination, so a comparison of the electron dynamics and harmonic emission throughout the recombination interval is straightforward. Addressing dynamics during ionization is more complicated, as the timing of ionization is inherently ill-defined for a quantum mechanical system. For the purpose of this study, we find a classical model of electron behavior in the driving field to be a sufficient approximation [3]. Using this picture, we assume that the electron acts as a point negative charge and is released from the molecule with  $z = \dot{z} = 0$  throughout the ionization interval of 9.75 – 10.0 field cycles. Assuming recombination to occur at the first instance when  $z = 0$ , each classical trajectory specifies a unique pair of ionization and recombination times (c.f. Fig. 2(g)). We then use the set of ionization times associated with recombination during the time interval of interest to analyze the electron dynamics during ionization. To characterize the nonadiabatic dynamics, we consider the variation of the phase difference  $\alpha$  which is presented at instants of ionization in Fig. 2(c,d) and of recombination in Fig. 2(e,f), respectively. Modifying the initial or return position of the electron within the internuclear distance does not alter the following analysis, since the internuclear distance is small in comparison to the quiver radius under the laser parameters of interest.

In the long wavelength case (Fig. 2(a)), the spectral minimum coincides with  $\alpha = 0$  at the time of ionization, but is not influenced by the behavior of  $\alpha$  during electron recombination. In contrast, for the shorter wavelength (Fig. 2(b))  $\alpha$  is not equal to zero throughout the ionization window and consequently suppressed harmonic generation is not observed. These short wavelength results let us conclude that the occurrence of  $\alpha = 0$  at the time of recombination does not lead to a suppression of harmonic emission. Thus, the minimum in the harmonic spectra is a spectroscopic signature of nonadiabatic electron dynamics exclusively at the time of ionization.

### B. Robustness of spectral signature

We expect that the modification of the HHG signal can be observed for a dissociating  $\text{H}_2^+$  molecule. Since the nonadiabatic behavior coincides with enhanced ionization [38, 39], regions with extended internuclear distances are expected to contribute dominantly to the total harmonic signal. We next examine the robustness of the signal to

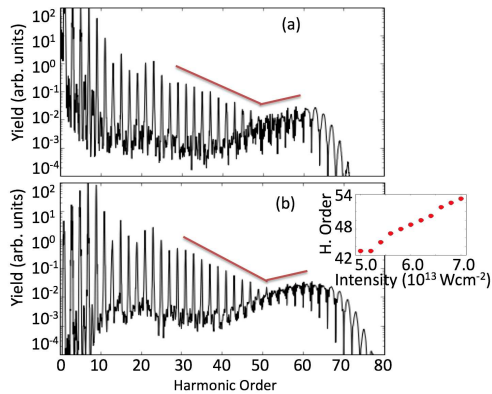


FIG. 3. (Color online) (a) The HHG spectrum calculated by integrating signals for fixed internuclear distances ( $R_0$ ) spanning 5.0–10.0 au maintains the spectral minimum for  $\lambda = 1.4 \mu\text{m}$ , intensity  $6 \times 10^{13} \text{ Wcm}^{-2}$ . (b) Fitting a distribution of laser intensities to a Gaussian beam profile, with maximum intensity  $7.0 \times 10^{13} \text{ Wcm}^{-2}$ , similarly maintains the minimum structure. The inset shows the linear dependence of the position of the spectral minimum with respect to the driving intensity, reflecting the non-structural nature of the causative mechanism.

variations of internuclear separation  $R_0$  (Fig. 3(a)), laser intensity (Fig. 3(b)), and carrier envelope phase. Near equilibrium, and for increasingly extended internuclear values ( $R_0 > 9.0$  au), ionization, and hence the HHG signal, is small. Furthermore, the HHG plateau remains flat. Consequently, the addition of these spectra does not influence the occurrence of the minimum. Other internuclear distances (for example,  $R_0 = 5.0$ ) contribute a spectral minimum at a similar harmonic frequency. Integration over internuclear distances spanning 5.0–10.0 a.u. in Fig. 3(a) therefore clearly exhibits the minimum.

In Fig. 3(b), we examine the effect of intensity variation by simulating an integrated HHG signal due to a Gaussian profile. At low intensities, we note that the transient localization of the electron does not take place. Consequently, spectra emitted by the system are flat throughout the plateau region, and contribute evenly to the total harmonic structure. As laser intensity increases, the spectral minimum appears and its position increases linearly with the laser intensity, as seen in the inset of Fig. 3(b). This linear behavior occurs since the ionization time interval at which  $\alpha = 0$  occurs remains rather invariant, while the corresponding recombination energy increases with the driving laser intensity. Thus, upon addition of harmonic spectra across this range with  $\Delta I = 0.2 \times 10^{13} \text{ Wcm}^{-2}$  in Fig. 3(b), the minimum remains apparent. Additional calculations have shown that the position of the minimum remains stable under variations of the carrier-envelope phase, which is expected. Although the temporal position of  $\alpha = 0$  events will shift with  $\phi$  according to Eq. (3), the peak of the electric field shifts by the same phase. As long as the duration of the laser field is sufficient, the presence and location of the

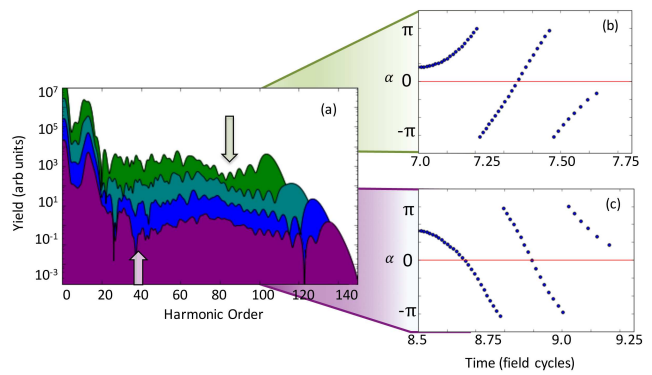


FIG. 4. (Color online) (left) Fourier transform of individual recombination events between 7.0-9.25 field cycles illustrates evolving electron dynamics (green, top: 7.0-7.75, teal: 7.5 - 8.25, blue: 8.0-8.75, purple, bottom: 8.5-9.25 field cycles; each spectrum shifted downward from predecessor by one order of magnitude). Using a  $2.0 \times 10^{14} \text{ Wcm}^{-2}$  driving laser, electron dynamics transitions between satisfying  $\alpha = 0$  once (top right) to twice (bottom right), resulting in the addition of a second minimum to the harmonic spectrum at low harmonic orders (left arrow) as the first minimum shifts to higher harmonic orders (right arrow).

minimum remains unchanged.

#### IV. IMAGING OF INTRAMOLECULAR ELECTRON DYNAMICS

We now explore the additional capacity for HHG to resolve changing intramolecular electron dynamics by performing windowed Fourier transforms of individual recombination events. This strategy mimics the experimental use of the attosecond lighthouse technique [40, 41] which imposes a temporal rotation of the instantaneous driving field wavefront, imparting angular separation to attosecond pulses emitted at different times. Through this technique, HHG generated from gases has been used to track the evolution of plasma formation and nonadiabatic dynamics in the generating medium [37], and similarly would be expected to provide an avenue to image the time-dependent electron dynamics ongoing within  $\text{H}_2^+$ .

By increasing the driving field strength to  $2.0 \times 10^{14} \text{ Wcm}^{-2}$ , we present a case where the transient localization of the electron dramatically modifies the spectral signal from one attosecond pulse to the next. At the peak of the driving field, we anticipate that the system will localize on the counterintuitive nucleus twice during the ionization window of HHG, resulting in two spectral minima. However, as the field ramps up throughout the first half of the laser pulse, we expose the electron to a changing effective intensity. The increasing magnitude of the electric field transitions the electron from an adiabatic regime to the nonadiabatic behavior of interest, and in particular provides the opportunity to image a changing number of localizations.

To resolve this progression, we show the spectral structure of several distinct rescattering events in Fig. 4(a). We begin in a regime in which  $\alpha = 0$  once at the time of ionization (green) as seen in Fig. 4(b) and depict the transition toward satisfying  $\alpha = 0$  twice during ionization (purple) shown in Fig. 4(c). Initially, we note only one spectral minimum, occurring at 83 harmonic orders and indicated by the rightmost arrow in Fig. 4(a). As the peak intensity at each cycle increases, this minimum shifts to higher energies in subsequent spectra. However, we also observe the formation of a second minimum beginning at 29 harmonic orders for recombination between 7.5 – 8.25 field cycles (teal). Initially, the second minimum corresponds to fulfilling  $\alpha = 0$  near the beginning of the recombination event starting at 7.5 field cycles. As intensity increases,  $\alpha = 0$  progressively later with respect to the beginning of each recombination event, shifting the minimum to 39 harmonic orders for recombination between 8.5 – 9.25 field cycles (left arrow). We envision this time-dependent behavior could be revealed through the use of the attosecond lighthouse technique, which would enable the separation of these rescattering events.

## V. CONCLUSIONS

We have identified a minimum in the HHG spectrum of  $H_2^+$  caused entirely by the behavior of the wave function at the time of tunnel ionization, rendering it novel in com-

parison with other minima observed in previous studies which contain information regarding the system during propagation or at the time of recombination. Our identification of this minimum links it directly to the nonadiabatic transient localization of the electron upon alternating nuclei, enabling us to trace the laser-driven manifestation of and changes to the nonadiabatic intramolecular dynamics of the electron through the emitted HHG signal.

## VI. ACKNOWLEDGEMENTS

M.M. acknowledges support by the National Science Foundation Graduate Research Fellowship under Grant No. DGE 1144083 and was also supported via a grant awarded by the U.S. Department of Energy Office of Basic Energy Science, Chemical Sciences, Geosciences and Biosciences Division, Atomic, Molecular and Optical Sciences Program (Award No. DE-FG02-09ER16103). A.J.-B. was supported by the U.S. National Science Foundation under Grant Nos. 1125844 and 1068706. A.B. acknowledges support by the U.S. Department of Energy Office of Basic Energy Science, Chemical Sciences, Geosciences and Biosciences Division, Atomic, Molecular and Optical Sciences Program (Award No. DE-FG02-09ER16103). This work utilized the Janus supercomputer, which is supported by the U.S. National Science Foundation (Grant No. CNS-0821794) and the University of Colorado Boulder.

- 
- [1] P.B. Corkum and F. Krausz, *Nat. Phys.* **3**, 381 (2007).
  - [2] T. Popmintchev, M.C. Chen, P. Arpin, M.M. Murnane, and H.C. Kapteyn, *Nat. Photon.* **4**, 822 (2010).
  - [3] P.B. Corkum, *Phys. Rev. Lett.* **71**, 1994 (1993).
  - [4] K.J. Schafer, B. Yang, L.F. DiMauro and K.C. Kulander, *Phys. Rev. Lett.* **70**, 1599 (1993).
  - [5] M.R. Miller, C. Hernandez-Garcia, A. Jaron-Becker, and A. Becker, *Phys. Rev. A* **90**, 053409 (2014).
  - [6] T. Popmintchev, M.-C. Chen, D. Popmintchev, P. Arpin, S. Brown, S. Alisaukas, G. Andriukaitis, T. Balciunas, O.D. Mücke, A. Pugzlys, A. Baltuska, B. Shim, S.E. Schrauth, A. Gaeta, C. Hernandez-Garcia, L. PLaja, A. Becker, A. Jaron-Becker, M.M. Murnane, and H.C. Kapteyn, *Science* **336**, 1287 (2012).
  - [7] M. Lein, *J. Phys B.: At. Mol. Opt. Phys* **40** R135 (2007).
  - [8] S. Baker, J.S. Robinson, C.A. Haworth, H. Teng, R.A. Smith, C.C. Chirila, M. Lein, J.W.G. Tisch, and J.P. Marangos, *Science* **312**, 424 (2006).
  - [9] N.L. Wagner, A. Wüst, I.P. Christov, T. Popmintchev, X. Zhou, M.M. Murnane, and H.C. Kapteyn, *Proc. Nat. Acad. Sci.* **103**, 13279 (2006).
  - [10] W. Li, X. Zhou, R. Lock, S. Patchkovskii, A. Stolow, H.C. Kapteyn, and M.M. Murnane, *Science* **322**, 1207 (2008).
  - [11] S. Baker, J.S. Robinson, M. Lein, C.C. Chirila, R. Torres, H.C. Bandulet, D. Comtois, J.C. Kieffer, D.M. Villeneuve, J.W.G. Tisch, and J.P. Marangos, *Phys. Rev. Lett.* **101**, 053901 (2008).
  - [12] H. Niikura, D.M. Villeneuve, and P.B. Corkum, *Phys. Rev. Lett.* **94**, 083003 (2005).
  - [13] O. Smirnova, Y. Mairesse, S. Patchkovskii, N. Dudovich, D. Villeneuve, P. Corkum, and M.Yu. Ivanov, *Nature* **460**, 08253 (2009).
  - [14] Z. Diveki, A. Camper, S. Haessler, T. Auguste, T. Ruchon, B. Carre, P. Salieres, R. Guichard, J. Caillat, A. Maquet, and R. Taieb, *New J. Phys.*, **14** 023062 (2012).
  - [15] H.J. Wörner, J.B. Bertrand, P. Hockett, P.B. Corkum, and D.M. Villeneuve, *Phys. Rev. Lett.* **104**, 233904 (2010).
  - [16] H.J. Wörner, J.P. Bertand, D.V. Kartashov, P.B. Corkum, and D.M. Villeneuve, *Nature* **466**, 604 (2010).
  - [17] H.J. Wörner, J.B. Bertrand, B. Fabre, J. Higuette, H. Ruf, A. Dubrouil, S. Patchkovskii, M. Spanner, Y. Mairesse, V. Blanchet, E. Mevel, E. Constant, P.B. Corkum and D.M. Villeneuve, *Science* **334**, 208 (2011).
  - [18] M. Lein, N. Hay, R. Velotta, J.P. Marangos, and P.L. Knight, *Phys. Rev. A* **66**, 023805 (2002).
  - [19] M. Lein, N. Hay, R. Velotta, J.P. Marangos, and P.L. Knight, *Phys. Rev. Lett.* **88**, 183903 (2002).
  - [20] M.F. Ciappina, A. Becker, and A. Jaron-Becker, *Phys. Rev. A* **76**, 063406 (2007).
  - [21] J. Itatani, J. Levesque, D. Zeidler, H. Niikura, H. Pepin, J.C. Kieffer, P.B. Corkum, and D.M. Villeneuve, *Nature* **432**, 867 (2004).

- [22] T. Kanai, S. Minemoto, and H. Sakai, *Nature* **435**, 470 (2005).
- [23] C. Vozzi, F. Calegari, E. Benedetti, J.P. Caumes, G. Sansone, S. Stagira, M. Nisoli, R. Torres, E. Heesel, N. Kajumba, J.P. Marangos, C. Altucci, and R. Velotta, *Phys. Rev. Lett.* **95**, 153902 (2005).
- [24] W. Boutu, S. Haessler, H. Merdij, P. Breger, G. Waters, M. Stankiewicz, L.J. Frasinski, R. Taieb, J. Caillat, A. Maquet, P. Manchicourt, B. Carre, and P. Salieres, *Nature Phys.* **4**, 545 (2008).
- [25] X. Zhou, R. Lock, W. Li, N. Wagner, M.M. Murnane, and H.C. Kapteyn, *Phys. Rev. Lett.* **100**, 073902 (2008).
- [26] C. Vozzi, M. Negro, F. Calegari, G. Sansone, M. Nisoli, S. De Silvestri and S. Stagira, *Nature Phys.* **7**, 822 (2010).
- [27] M. Spanner, J. Mikosch, A. Gijsbertsen, A.E. Boguslavskiy and A. Stolow, *New J. Phys.* **13**, 093010 (2011).
- [28] I. Kawata, H. Kono, and Y. Fujimura, *Chem. Phys. Lett.* **289**, 546 (1998).
- [29] Y.-C. Han and L. B. Madsen, *Phys. Rev. A* **87**, 043404 (2013).
- [30] I. Kawata, H. Kono, and Y. Fujimura, *J. Chem. Phys.* **110**, 11152 (1999).
- [31] N. Takemoto and A. Becker, *Phys. Rev. Lett.* **105**, 203004 (2010).
- [32] M. Odenweller, N. Takemoto, A. Vredenburg, K. Cole, K. Pahl, J. Titze, L.Ph.H. Schmidt, T. Jahnke, R. Dörner, and A. Becker, *Phys. Rev. Lett.* **107**, 143004 (2011).
- [33] M. Lezius, V. Blanchet, D.M. Rayner, D.M. Villeneuve, A. Stolow, and M.Yu. Ivanov, *Phys. Rev. Lett.* **86**, 51 (2001).
- [34] M. Lezius, V. Blanchet, M.Yu. Ivanov, and A. Stolow, *J. Chem. Phys.* **117**, 1575 (2002).
- [35] A.N. Markevitch, S.M. Smith, D.A. Romanov, H.B. Schlegel, M.Yu. Ivanov, and R.J. Levis, *Phys. Rev. A* **68**, 011402(R) (2003).
- [36] N. Takemoto and A. Becker, *J. Chem. Phys.* **134**, 074309 (2011).
- [37] K.T. Kim, C. Zhang, T. Ruchon, J.-F. Hergott, T. Auguste, D.M. Villeneuve, P.B. Corkum and F. Quéré, *Nature Photon.* **7**, 651-656 (2013).
- [38] T. Zuo and A.D. Bandrauk, *Phys. Rev. A* **52**, R2511 (1995).
- [39] T. Seideman, M.Y. Ivanov, and P.B. Corkum, *Phys. Rev. Lett.* **75**, 2819 (1995).
- [40] H. Vincenti and F. Quéré, *Phys. Rev. Lett.* **108**, 113904 (2012).
- [41] J.A. Wheeler, A. Borot, S. Monchocé, H. Vincenti, A. Ricci, A. Malvache, R. Lopez-Martens, and F. Quéré, *Nature Photon.* **6**, 829-833 (2012).